Paper

Visual Simulation of Solar Photosphere Based on Magnetohydrodynamics and Quantum Theory

Tomokazu ISHIKAWA†, Yonghao YUE† (Member),
Yoshinori DOBASHI†† (Member), Tomoyuki NISHITA† (Member)
† The University of Tokyo
†† Hokkaido University

⟨Summary⟩ We propose an efficient method based on physical laws to model phenomena near the surface of the sun, which is known as the solar photosphere. In the field of astronomy, some physical models have been developed to simulate the sun's turbulence. Most of the previous models are difficult to be applied in the making of CG images since they require a considerable amount of time even when using a supercomputer. The subject of our research is the visual simulation of the phenomena observed above the photosphere, namely solar prominences, because these are characteristic phenomena of the sun that can greatly influence the visual impact in movies and games.The sun is mainly composed of ionized plasma, and its behavior can be treated as a fluid. However, unlike gas, the plasma fluid is influenced by the magnetic field. Thus, magnetic field calculations are needed to calculate the plasma behavior. We use the magnetohydrodynamics (MHD) equations to simulate the behavior of plasma. We propose a new method which can simulate a prominence in a practical computation time. The computation cost is reduced by simplifying the phenomena inside the sun: we only consider the phenomena after the solar prominence erupts because the phenomena before the eruption dose not manifest itself in a visual way. To render the simulation results, we emulate an observation method that extracts the specific spectrum emission from the solar plasma.

Key words: Solar phenomenon, Plasma simulation, Magnetohydrodyanamics

1. Introduction

Visualization methods of planets, for example Jupiter[1)] and the Earth[2)3)], have been researched, and are being used to create images for commercial films, movies, and computer games. However, visual simulation method for the sun has not been developed in the field of CG. Among the various phenomena associated with the sun (see Fig. 1), we simulate solar prominences because they are observable and distinguishable features features above the sun's surface.

In a conductor such as a plasma fluid, the magnetic field changes and electric current is generated, due to the fluid flow. Consequently, interaction between the electric current and the magnetic field exerts an external force on the plasma fluid. Such complex behavior

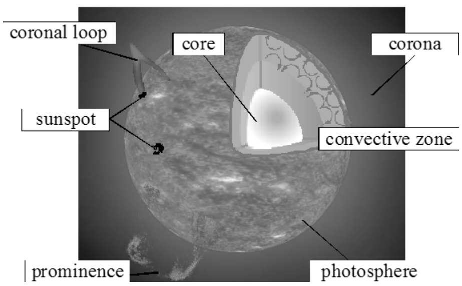

Fig. 1 Various phenomena of the sun.

is described by the MHD equations.

Although it is possible to simulate the entire plasma fluid inside and outside the sun with the complex behavior in consideration, its computation cost is too expensive for an application in the CG field even when using a supercomputer. In this paper, we propose a new simulation model for the solar prominence subjected to practical applications in the CG field. The computation cost is reduced mainly by simplifying the phenomena inside the sun: we do not try to simulate the trigger of the solar prominence but simulate the solar prominence after it is triggered. We believe that this simplification is acceptable for applications in the CG field because the phenomena inside the sun cannot be observed. We focus on the physically based simulation above the sun, and use magnetic field lines and particles to represent the fine structure of the solar prominence, which is difficult to be captured using a coarse grid.

For rendering, we calculate the specific wavelength that the plasma emits and as used in astronomy, its intensity is converted to RGB colors using a pseudo-color.

2. Related Work

Fluid simulation is one of the important research fields in CG. Stam proposed a stable technique for simulating fluid motion even when the timestep is large by using a semi-Lagrangian advection scheme to calculate the advection term in the Navier-Stokes equations[4]. Fedkiw et al. introduced a technique called vorticity confinement to model small scale vortices that cannot be represented by the simulation with coarse grids[5]. Not only the behavior of the fluid but also the interaction of the plasma fluid and the magnetic field is important in the sun. Though the technique for simulating the magnetic field was proposed by Thomaszewski et al.[6], only the magnetism of rigid bodies is calculated as an influence of magnetic fields. The research to calculate the interaction of the magnetic field to the fluid has not been developed in the field of CG.

Baranoski proposed a visual simulation method of the aurora by means of simulating the interaction between electrons and the magnetic field using particles with electrical charge[7][8]. In these researches, the change of the magnetic field by the influence of electrically charged particles and magnetic field generated by astronomical objects such as the earth is not considered. Therefore, it is not possible to apply these methods to the motion of the fluid on sun surface where the change in the magnetic field causes important effect.

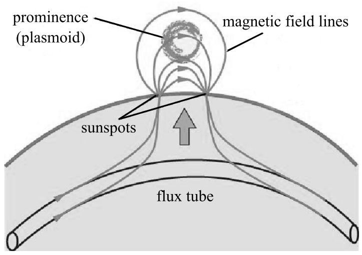

Fig. 2 Sun's magnetic field and mechanism of prominences.

We add magnetic field and temperature to the elements of fluid simulation based on the semi-Lagrangian advection scheme. Furthermore, we assume the fluid to be incompressible for stable simulation.

3. Solar Prominence

A prominence is a phenomenon in which a mass of plasma is ejected as far as 350,000 km from the sun's surface.

A prominence is caused by changes in the magnetic field structure of the sun. The magnetic field rises from the surface due to the differential rotation of the sun[9]. A mass of plasma known as a plasmoid rises from the surface of the sun (see Fig. 2).

Thus, the time evolution of the magnetic field is an important factor in simulating the prominences.

4. Our Simulation Method

4.1 Governing equations

The plasma fluid in the sun has a very small electrical resistance and we can use an approximation known as the ideal MHD approximation. In our simulation, the following MHD equations and the time evolution of the temperature are used.

$$\nabla \cdot \mathbf{u} = 0, \quad (1)$$

$$\frac{\partial \mathbf{u}}{\partial t} + (\mathbf{u} \cdot \nabla)\mathbf{u} = -\nabla p + \nu \nabla^2 \mathbf{u} + \mathbf{j} \times \mathbf{B} + 2\mathbf{\Omega} \times \mathbf{u}, \quad (2)$$

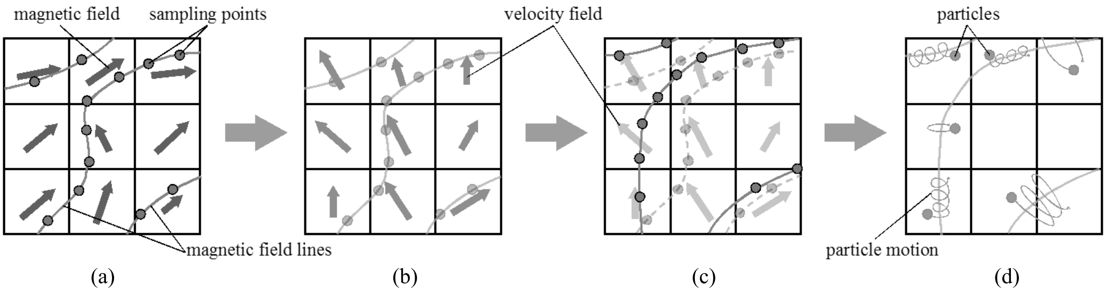

Fig. 3 Overview of our method. (a) Reconstruct the magnetic field vector in each voxel from magnetic field vectors of sampling points. (b) Update the velocity field according to the Navier-Stokes equations. (c) Advect each sampling point of magnetic field lines. (d) Move particles due to the Lorentz force.

$$\frac{\partial \mathbf{B}}{\partial t} = -\nabla \times \mathbf{E} = \nabla \times (\mathbf{u} \times \mathbf{B}), \tag{3}$$

$$\frac{\partial T}{\partial t} + (\mathbf{u} \cdot \nabla)\, T = \nabla^2 T, \tag{4}$$

where $\mathbf{u}$ is the velocity vector, p is the pressure, ν is the kinematic viscosity, $\mathbf{j}$ is the electric current density. $\mathbf{j}$ can be replaced with the rotation of the magnetic field by Ampere's rule,

$$\mathbf{j} = \frac{1}{\mu} \nabla \times \mathbf{B}. \tag{5}$$

$\mathbf{B}$ is the magnetic field. μ is the magnetic permeability and we use $\mu = 4\pi \times 10^{-7}$. In a rotating astronomical body like the sun, we must consider the Coriolis force as an external force in computing the velocity field. The forth term on the right hand side of Equation (2) corresponds to the Coriolis force and $\Omega = (0, \omega \cos\varphi, \omega \sin\varphi)$ is the angular velocity vector where φ is the latitude and $\omega = 0.01034$ rad/s is the rotation rate of the sun. Equation (3) represents the time evolution of the magnetic field $\mathbf{B}$. $\mathbf{E}$ is the electric field and the right hand side of Equation (3) is derived from Ohm's law and the assumption that the plasma has very small electrical resistance. Equation (4) represents the time evolution of the temperature T.

4.2 Overview

The equations described above consist of the Navier-Stokes equations (Equations (1) and (2)) and the Maxwell equations (Equations (3)). To solve the Navier-Stokes equations, we used the solver proposed by Stam[4]. We propose a method to solve Maxwell equations.

To simulate the evolution of solar prominences, the velocity field, the magnetic field, and the temperature field are necessary. These physical quantities other than the magnetic field are stored in the voxels, and updated by the results of numerical analysis based on the ideal MHD equations. The magnetic field is updated by using the magnetic field lines (please see Section 4.3 for the details). The simulation space is restricted to the domain containing the prominence ejection, and represented using orthogonal coordinates. Moreover, a set of particles are generated in order to compute the evolution of the plasma fluid. The particles have positions and velocities, and are subject to Lorentz force from the magnetic field.

Fig. 3 shows the basic concept of a process at each timestep in the simulation. We define the magnetic field lines according to the initial state (please see Section 4.6 for the details) of magnetic field. Next, the velocity field is updated by calculating the Navier-Stokes equations (see Fig. 3 (b)). The magnetic field lines are advected along the updated velocity field (see Fig. 3 (c)). The particles and temperature are also advected. For each particle, the Lorentz force is calculated and particle position is updated (see Fig. 3 (d)). During the rendering process, we calculate particle colors based on the intensity of the specific spectrum.

4.3 Magnetic field lines

To update the magnetic field, we do not use the voxel representation; instead, we use line segments along the magnetic field vector. The line segments enable us to represent the magnetic field topology more efficiently than using a large number of voxels. Our method can handle the complex magnetic field, which is not possible to be represented by using coarse voxels.

In the field of physics, the magnetic field lines are only used to visualize the magnetic field and they have no meanings in the simulation. However in our method, they are used to represent the magnetic field. We define the *magnetic field lines* by parametric curves $\mathbf{x}_P$ generated from the magnetic vector field, which is given by the following equations,

$$\frac{d\mathbf{x}_P(\theta)}{d\theta} = \mathbf{B}_P(\mathbf{x}_P(\theta)), \tag{6}$$

$$\mathbf{x}_P(\theta_0) = \mathbf{x}_{P_0}, \tag{7}$$

where $\mathbf{B}_P$ is the magnetic field vector of the sampling point P on parametric curves $\mathbf{x}_P$, which is parameterized by θ. $\mathbf{B}_P$ is stored in each sampling point. $\mathbf{x}_{P_0}$ is the starting position of the magnetic field line. These equations correspond to the streamline when the magnetic field is assumed to be a velocity field. The starting points in the stream lines are the centers of voxels at the boundary of the simulation space.

A sufficient number of magnetic field lines are calculated to reconstruct the initial magnetic field given as voxel data. The magnetic field lines are subdivided into small segment dx and the sampling points are generated. Thus, the magnetic field lines are represented by a set of connected sampling points. We use the following equation to reconstruct the magnetic field from the sampling points:

$$\mathbf{B}^*(\mathbf{x}) = \sum_P W(\mathbf{x} - \mathbf{x}_P)\mathbf{B}_P, \tag{8}$$

where $\mathbf{B}^*$ is the reconstructed magnetic field, W is a kernel function defined as,

$$W(\mathbf{x}-\mathbf{x}_P) = \begin{cases} w \cdot \exp(\frac{-\|\mathbf{x}-\mathbf{x}_P\|^2}{2r^2}) & (\|\mathbf{x} - \mathbf{x}_P\| \leq r) \\ 0 & (otherwise), \end{cases} \tag{9}$$

where w is a user-specified weighting factor, r is an influence radius. We use $w = 0.8$ and set r to one-tenth to the longest width of the simulation space.

Note that the definition of our magnetic field lines stated above is different from that in the physics. Our magnetic field lines are developed for efficient representation and fast reconstruction of the magnetic field, whereas the magnetic field lines appearing in physics are used for easily understandable visualization by putting more lines in regions with stronger magnetism.

4.4 Time evolution of magnetic field

Equation (3) for the evolution of the magnetic field is rewritten in the following way:

$$\frac{\partial \mathbf{B}}{\partial t} = (\mathbf{B}\cdot\nabla)\mathbf{u} - (\mathbf{u}\cdot\nabla)\mathbf{B} + \mathbf{u}(\nabla\cdot\mathbf{B}) - \mathbf{B}(\nabla\cdot\mathbf{u}). \tag{10}$$

The third term of Equation (10) is zero according to Gauss's law for magnetism of the Maxwell's equations, and the fourth term is zero using Equation (1). Therefore, we can further rewrite Equation (10) as

$$\frac{\partial \mathbf{B}}{\partial t} + (\mathbf{u} \cdot \nabla)\mathbf{B} = (\mathbf{B} \cdot \nabla)\mathbf{u}. \tag{11}$$

The second term of the left hand side in Equation (11) is an advection term, so the sampling points on the magnetic field lines are moved according to the velocity field. The right hand side of Equation (11) is a stretching term due to the velocity field.

4.5 Motion of plasma particles

We use the particles to calculate the detailed motion of the plasma including rotation motion caused by Lorentz force. The particles are also used to render the simulation results. Each particle represents a fraction of plasmoid. These particles are advected along the velocity field and their colors are calculated from the temperature field. The particles have electric charge, and are subject to the Lorentz force calculated from the magnetic field. As just advecting particles along the velocity field updated by using the coarse grid, we cannot express twist of prominences. Therefore, we apply the Lorentz force to particles to reproduce the fine movement (see section 6 for more details). The Lorentz force affects the update of the velocity field and the motion of particles. Therefore, the equation of motion of the particles can be written as follow:

$$\frac{d\mathbf{v}}{dt} = \frac{q}{m}(\mathbf{v} \times \mathbf{B}), \tag{12}$$

where $\mathbf{v}$ is the velocity vector of the particle, q/m is charge/mass ratio. $\mathbf{v}$ is determined by updating using Equation (12) and interpolating the voxel data $\mathbf{u}$.

4.6 Initial condition of prominence simulation

We refer to research results in astronomy[10] to determine the initial condition of the magnetic field lines, because it is difficult to obtain real data for the magnetic field of the sun. We determine the initial magnetic field and velocity field in the normalized simulation space by using the following equation,

$$\mathbf{u} = (0, u\cos(\pi(x - x_{mid})), 0),\ 0 \leq x \leq 1, \tag{13}$$

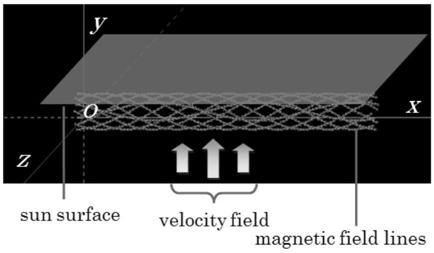

Fig. 4 Initial state of prominence simulation.

Table 1 Parameter setting of prominence simulation.

parameter	meaning	value	unit
dt	time step	0.01	hour
d	voxel width	3.0×10^3	km
u	magnitude of velocity in Equation (13)	1.8×10^3	km/h
$B_{photosphere}$	magnetic field strength in the photosphere in Equation (14)	2000	G
B_{corona}	magnetic field strength above the photosphere in Equation (14)	26	G
$T_{photosphere}$	temperature for an enviromental value in the photosphere	6.0×10^4	K
T_{corona}	temperature for an enviromental value above the photosphere	1.0×10^6	K

$$\mathbf{B} = \begin{cases} \begin{pmatrix} B_{corona} \\ 0 \\ 0 \end{pmatrix} & (h_{sur} < y) \\ \begin{pmatrix} B_{photosphere} \\ \frac{z-z_c}{\sqrt{(y-y_c)^2+(z-z_c)^2}} \\ \frac{y-y_c}{\sqrt{(y-y_c)^2+(z-z_c)^2}} \end{pmatrix} & (0 < y \leq h_{sur}), \end{cases} \quad (14)$$

where u is the magnitude of the velocity, x_{mid} is the center of the inflow of velocity field. and B_{corona}, $B_{photosphere}$ is the magnetic field strength above/in the photosphere, respectively. We define the height of the photosphere in the simulation space by $h_{surface}$. y_c and z_c are the center of the magnetic field lines.

The parameters used for the simulation shown in this paper are summarized in Table 1. We show the initial state for simulating a solar prominence in Fig. 4. The magnetic field is updated by directly moving the sampling points on the magnetic field lines according to the velocity field.

Although, in reality, the magnetic field lines beneath the sun's surface rise due to the differential rotation of the sun, we simply set an upward velocity field as the initial condition for the velocity field so that the magnetic field lines can rise (see Fig. 4). Every particle is uniformly generated under the sun's surface. The prominence is observed as the particles are lifted up along to the velocity field.

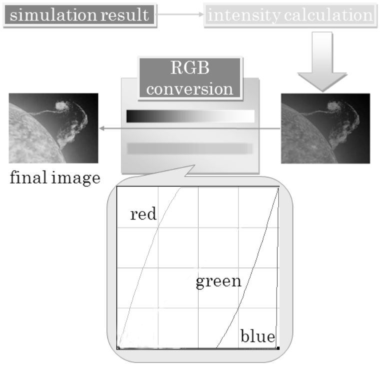

Fig. 5 Our rendering process. First, we calculate the intensity of the Hα spectrum at each particle according to its temperature. Then, the intensity is converted into RGB colors by using the color table which astronomers use. (Note that in the printed version of this paper, the colors appear to be grayscale.)

5. Rendering

The solar prominences are observed by extracting Hα spectrum. In the field of astronomy, the observed images (original images are in grayscale) are colored according to the intensity of plasma emission by using a programming language "IDL" [11]. Fig. 5 shows our rendering process. During the rendering process, the intensity plasma emits is calculated and converted into RGB by referring to the color table which astronomers use. We use the RGB conversion function represented by tone curve as shown in the Fig.5.

The solar prominence colors in the final images are determined from the intensity of the Hα spectrum. The visible spectrum of light from hydrogen displays four wavelengths, 410.17 nm (violet), 434.05 nm (blue), 486.13 nm (blue-green), and 656.28 nm (red). The wavelength of 656.28 nm is the Hα spectrum.

While the black body radiation can be used to calculate the intensity of solar photosphere, the Hα spectrum is mainly due to the emission process of hydrogen plasma, which is determined through quantum mechanics. The solar prominence cannot be considered as a perfectly black body, because the solar prominence is mainly composed of hydrogen plasma.

Hα spectrum is emitted due to the photoelectric effect when the energy level of hydrogen atoms moves

Table 2 Numerical error between the magnetic field simulated by using magnetic field lines and that by using voxels
time unit: s, distance unit: m, error unit: %

$dx \setminus dt$	0.1	0.01	0.001
1.00	1.5831	0.8309	0.8516
0.50	0.5274	0.2538	0.2595
0.25	0.2328	0.1296	0.1372

(a) unidirectional flow

$dx \setminus dt$	0.1	0.01	0.001
1.00	23.3682	7.4897	1.3763
0.50	11.4603	3.2574	0.5988
0.25	6.5817	2.8531	0.4054

(b) vortex flow

from an upper level 3 to a lower level 2. This transition occurs stochastically, and its probability is known as the Einstein's A coefficient for emission [12]. The intensity of Hα spectrum $I_{H\alpha}$ is calculated by the following equation, considering absorption and the induced emission.

$$I_{H\alpha} = \frac{h\nu_{H\alpha}L}{4\pi}\frac{N_3 A_{32}}{N_3 B_{32} - N_2 B_{23}}, \tag{15}$$

where h is Planck's constant, $\nu_{H\alpha}$ is the frequency of emitted light, L is the thickness of plasma, N_i is the number of atoms of the energy level i, A_{32} is Einstein's A coefficient when the energy level moves from 3 down to 2. B_{23} and B_{32} are the Einstein's B coefficients for absorption and induced emission respectively (see appendix for details). The existence probability of the atoms of energy level i is calculated from Boltzmann principle[13],

$$\frac{N_i}{N} = \frac{g_i \exp(-E_i/kT)}{u(T)}, \tag{16}$$

where N is the total number of atoms, N_i is the number of the atoms of energy level i, g_i is the degeneracy of energy level i (In case of a hydrogen atom made from spinless particles, g_i is i^2 [14].), E_i is the energy level i, k is Boltzmann's constant. T is the temperature obtained from Equation (4). $u(T)$ is called partition function and defined as the following equation [15],

$$u(T) = \sum_i g_i \exp(-E_i/kT). \tag{17}$$

6. Results

In this section, we first present a validation of our approach using the magnetic field lines, then show the simulation results of the solar prominence.

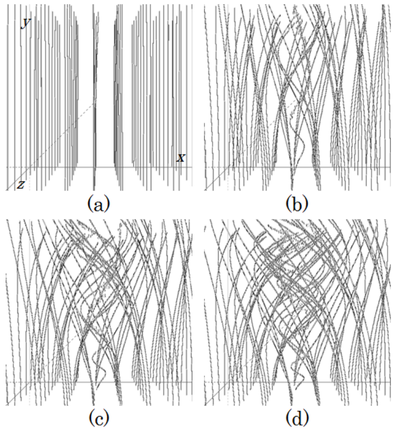

Fig. 6 Simulation results of magnetic field lines evolution in velocity field of vortex.

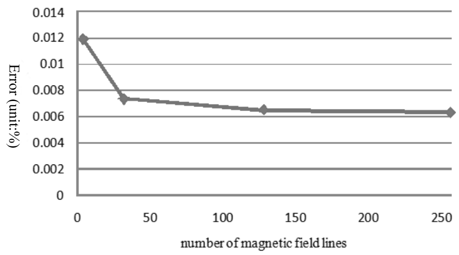

Fig. 7 Simulation results of magnetic field lines evolution in velocity field of vortex.

6.1 Validation of our approach using the magnetic field lines

In the traditional approach for computing the magnetic field, the field is represented as a form of volume data and sampled at voxel centers. On the other hand, our method represents the magnetic field by a set of magnetic field lines and the evolution of the lines is calculated. In order to demonstrate the validity of our approach, we compare our results with results using the traditional voxel-based approach. The evolution of the magnetic field is calculated for two different kinds of simple velocity fields. One is a unidirectional flow (toward the positive of the x axis.) and the other is a vortex. The velocity field of a vortex is decided by the following equation,

$$\mathbf{u} = \begin{pmatrix} \frac{ay^2(z-z_c)}{(x-x_c)^2+(z-z_c)^2} \\ 0 \\ \frac{by^2(x-x_c)}{(x-x_c)^2+(z-z_c)^2} \end{pmatrix}, \tag{18}$$

where, $a = -0.1$ and $b = 0.1$ are constants of vortex strength, x_c and z_c are position of vortex center, In this experiment, the velocity field is fixed. We compute RMS error between the voxel data converted from magnetic field lines and the simulating data by using voxels. Fig. 6(a) shows the initial state of the experiment. In Fig. 6, the gray lines are magnetic field lines, which are initially set perpendicular to the xz plane. Figs. 6(b) to (d) show the results of magnetic field lines transformed by the velocity field based on Equation (18). Tables 2(a) and (b) show the results of the experiments which are simulated under the settings of the initial velocity fields being unidirectional flow and vortex flow, respectively. The numerical value is the RMS error after 100 time steps. dx is the sampling interval of magnetic field lines, shown in the ratio to the width of a unit voxel, and dt is the time step of the simulation. The number of grid points is $64 \times 64 \times 64$. From Table 2, we can see that the error becomes smaller as dx or dt are set smaller. This error is small enough and the variance is also small. Therefore we can accurately simulate the time evolution of the magnetic field by using magnetic field lines instead of the voxels. Moreover, our method can handle the complex magnetic field including the twist of magnetic field lines, which is not possible to be represented by using coarse voxels. Fig. 6(d) shows magnetic field lines after 90 time steps of the simulation with the velocity field initialized to form a vortex. The twist of magnetic field lines can be simulated as shown in Fig. 6(d).

Fig. 7 shows the relationship between numerical errors and the number of magnetic field lines while dx and dt are fixed.

6.2 Simulation results of the solar prominence

We map the texture based on an observed image on the sun's surface and the corona is also displayed by mapping the texture based on a Gaussian distribution.

We compare the magnetic field calculated by using magnetic field lines with results using volume data. Fig. 8 shows the comparison between results using our method and voxel based simulation to calculate the time evolution of magnetic field. Our method can simulate the complex behavior of the plasma including rising and twisting of the plasma around magnetic field lines. This twisting effect is the result of adding the Lorentz force to the particles.

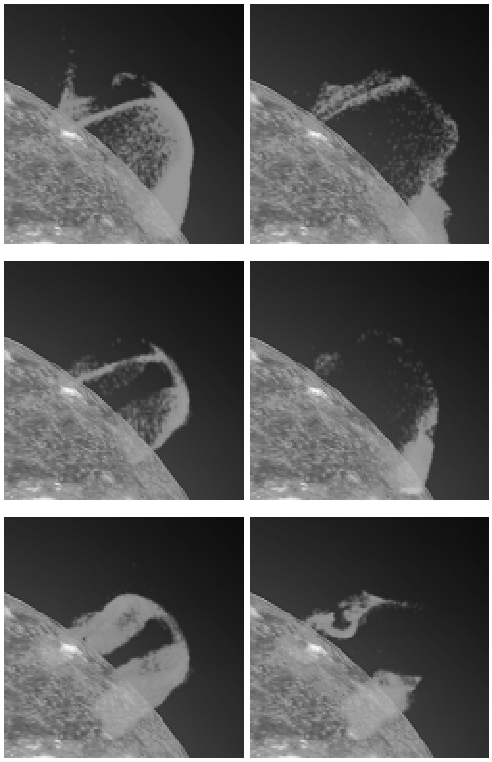

Fig. 8 Comparison between results using voxel based simulation (top) and using our method (middle). Bottom shows the results with Lorentz and Coriolis forces applied to our method.

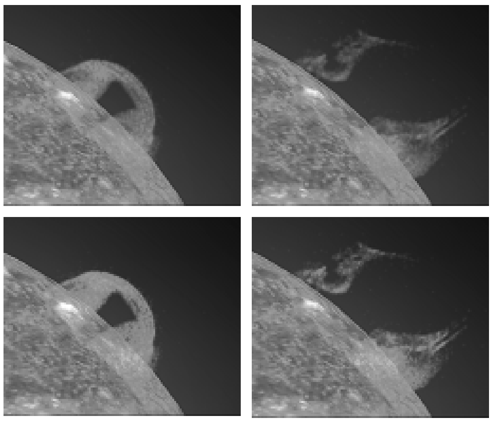

Fig. 9 Comparison of the intensity calculations. Calculation result of the intensity based on black body radiation (top) and emission process of hydrogen plasma (bottom).

We compare the result of the emission process and the result of the black body radiation. The intensity

B_λ of the black body radiation is calculated from the Planck distribution function.

$$B_\lambda(T) = \frac{2\pi hc^2}{\lambda^5} \frac{1}{\exp(hc/\lambda kT) - 1}, \tag{19}$$

where λ is the wavelength and c is the speed of light. Fig. 9 shows the results of the intensity by the black body radiation and the emission process. It is necessary to consider the emission process when the temperature of the objects is high, such as plasma. Fig. 10 shows the prominence simulated by our method, which is lifted from the photosphere. Figs. 10 (a) to (d) are the results for 100 to 190 minutes. The simulation space where the prominence erupts is subdivided into a grid.

The resolution of the grid is 64 × 128 × 64. We use 10 magnetic field lines and each magnetic field line is subdivided into 960 sampling points. The average computation time per a single timestep is 3 seconds on a standard PC (CPU: Core i7 3.2GHz, RAM: 12.0GB). We can synthesize the shape of the prominence that is similar to the real prominence by adding Lorentz and Coriolis forces as the external force.

Fig. 11 shows appearance of the prominence when viewed from two different viewpoints. Fig.12 shows the comparison between the result using our method and a satellite image taken by NASA.

Fig. 13 shows images of the simulation results of the entire sun. Figs. 10 (a) to (d) are the results for 100 to 280 minutes. The evolution of the prominence depends on the latitude, since the Coriolis force is determined by the latitude. In these simulations, one timestep corresponds to approximately 2 minutes.

7. Conclusions and Future Work

We have proposed an efficient method for the time evolution of a magnetic field, and have shown its application to solar prominences. Taking into account the MHD equations, we can simulate the behavior of a plasma fluid. Our method is able to render the sun by calculating the specific wavelength actually observed.

For future work, we are planning to implement our method on the GPU and to develop a stable simulation method including a magnetic reconnection.

As we focused on physical-based simulation of prominences, we merely used simple texture mapping to represent the corona and supergranulation (a particular pattern on the sun's surface). We plan to propose models for these phenomena as well as for flares (the explosive phenomenon observed above the photosphere).

References

1) L. Yaeger and C. Upson, "Creation of the planet jupiter for the film 2010," in *SIGGRAPH '86: ACM SIGGRAPH 1986*, pp. 85–93, 1986.
2) T. Nishita, T. Shirai, T. Katsumi, and E. Nakamae, "Display of the earth taking into account atmospheric scattering," in *SIGGRAPH '93: ACM SIGGRAPH 1993*, pp. 175–182, 1993.
3) Y. Dobashi, T. Yamamoto, and T. Nishita, "A controllable method for animation of earth-scale clouds," in *CASA 2006*, pp. 43–52, 2006.
4) J. Stam, "Stable fluids," in *SIGGRAPH '99: ACM SIGGRAPH 1999*, pp. 121–128, 1999.
5) R. Fedkiw, J. Stam, and H. W. Jensen, "Visual simulation of smoke," in *SIGGRAPH '01: ACM SIGGRAPH 2001*, pp. 15–22, 2001.
6) B. Thomaszewski, A. Gumann, S. Pabst, and W. Strasser, "Magnets in motion," in *SIGGRAPH '08: ACM SIGGRAPH 2008*, pp. 162:1–162:9, 2008.
7) G. Baranoski, J. Rokne, P. Shirley, T. Trondsen, and R. Bastos, "Simulation the aurora," *Visualization and Computer Animation*, vol. 14, no. 1, pp. 43–59, 2003.
8) G. Baranoski, J. Wan, J. Rokne, and I. Bell, "Simulating the dynamics of auroral phenomena," *ACM Transactions on Graphics (TOG)*, vol. 24, no. 1, pp. 37–59, 2005.
9) H. Isobe, T. Miyagoshi, K. Shibata, and T. Yokoyama, "Filamentary structure on the sun from the magnetic rayleigh-taylor instability," *Nature*, vol. 434, pp. 478–481, 2005.
10) K. Nishida, M. Shimizu, D. Shiota, H. Takasaki, T. Magara, and K. Shibata, "Numerical examination of plasmoid-induced reconnection model for solar flares," *The Astrophysical Journal*, vol. 690, pp. 748–757, 2009.
11) C. Markwardt, "Unofficial format specification of the idl," 11 2009.
12) J. Wilson and J. F. B. Hawkes, *Lasers: Principles and Applications*. Prentice Hall, 1987.
13) M. N. Saha, "On a physical theory of stellar spectra," in *Royal Society of London*, pp. 135–153, 1921.
14) I. H. Duru and H. Kleinert, "Solution of the path integral for the h-atom," *Physics Letters B*, vol. 84(2), pp. 185–188, 1979.
15) E. Prati, M. Belli, M. Fanciulli, and G. Ferrari, "Measuring the temperature of a mesoscopic electron system by means of single electron statistics," *Applied Physics Letters*, vol. 96, pp. 1–9, 2010.
16) Q. A. Wang and A. L. Méhauté, "Nonextensive blackbody distribution function and einstein's coefficients a and b," *Physics Letters A*, vol. 242, pp. 301–306, 1998.

Appendix A Einstein's A coefficient

The Einstein's A coefficient is the spontaneous transition probability from an energy level to another level and is calculated by means of perturbation the-

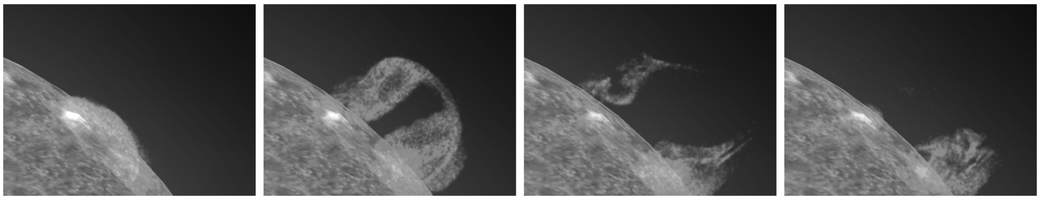

(a) t = 100 min (b) t = 130 min (c) t = 160 min (d) t = 190 min

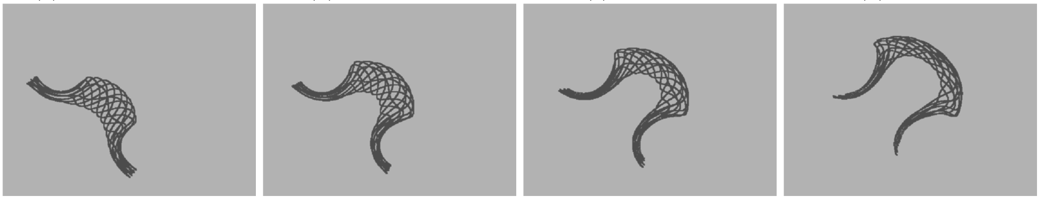

(e) t = 100 min (f) t = 130 min (g) t = 160 min (h) t = 190 min

Fig. 10 Simulation results of erupting prominence. (a) to (d) are final images created by our method. (e) to (h) are distribution of magnetic field lines corresponding to (a) to (d), respectively.

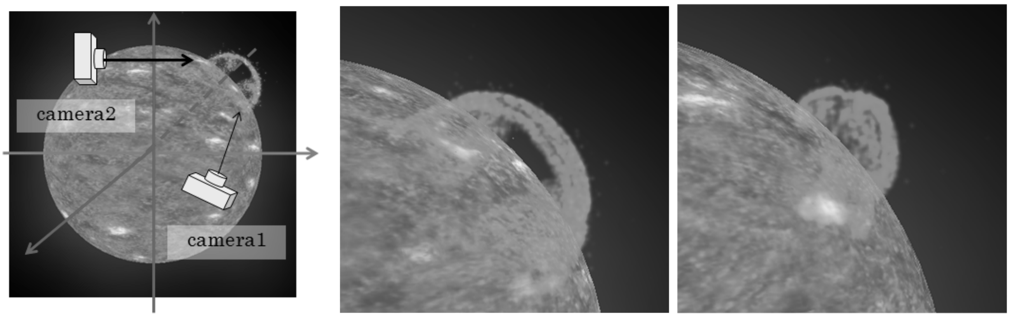

(a) view from camera1 (b) view from camera2

Fig. 11 Result images of changing the viewpoint.

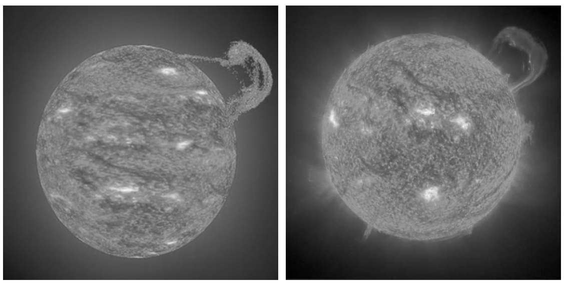

(a) our result (b) observation by NASA

Fig. 12 Comparison between our result and the actual phenomena above the sun.

ory of quantum mechanics. We use the perturbation term $H'(x,\ t)$ defined by Equation (A1). $H(t)$ is a time-dependent Hamiltonian. The Einstein's A coefficient is given by Equation (A2) which can be induced from Schrodinger equation.

$$H(t) = H_0 + H'(x,t) = H_0 + x^2 e^{-t}, \qquad \text{(A1)}$$

$$A_{32} = \frac{4\pi^2}{h}\Big|\int_{-\infty}^{\infty} \langle n=2|H'(x,t)|n=3\rangle e^{i\omega_{32}t}dt\Big|^2, \text{(A2)}$$

where H_0 is the unperturbed Hamiltonian, $\omega_{32} = 2\pi(E_3 - E_2)/h$, $|n = i>$ is a vector of the wave function $f_i(x)$ that corresponds in energy level i. E_i is the energy level i and h is Planck's constant.

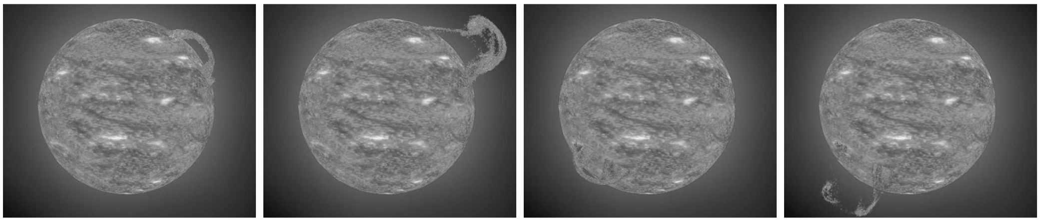

(a) t = 100 min (b) t = 160 min (c) t = 220 min (d) t = 280 min

Fig. 13 Simulation results of erupting prominence - entire picture of the sun -

We can obtain B_{ij} and B_{ji} in Equation (15) from A_{ij} as follows,

$$B_{ij} = \frac{c^3}{8\pi h\nu_{ij}^3} A_{ij}, \quad \text{(A3)}$$

$$B_{ji} = \frac{g_i}{g_j} B_{ij}. \quad \text{(A4)}$$

In Equation (A3), ν_{ij} is the frequency of emitted light when the energy level moves from i down to j. The above Equations (A3) and (A4) hold at any temperature[16).

(Received Jul. 16, 2010)
(Revised Jan. 7, 2011)